



CHORUS

This is the accepted manuscript made available via CHORUS. The article has been published as:

Negative Quasiprobabilities Enhance Phase Estimation in Quantum-Optics Experiment

Noah Lupu-Gladstein, Y. Batuhan Yilmaz, David R. M. Arvidsson-Shukur, Aharon Brodutch, Arthur O. T. Pang, Aephraim M. Steinberg, and Nicole Yunger Halpern

Phys. Rev. Lett. **128**, 220504 — Published 2 June 2022

DOI: [10.1103/PhysRevLett.128.220504](https://doi.org/10.1103/PhysRevLett.128.220504)

Negative quasiprobabilities enhance phase estimation in quantum-optics experiment

Noah Lupu-Gladstein,^{1,*} Y. Batuhan Yilmaz,^{1,†} David R. M. Arvidsson-Shukur,^{2,3,‡} Aharon Brodutch,^{1,§} Arthur O. T. Pang,^{1,¶} Aephraim M. Steinberg,^{1,**} and Nicole Yunger Halpern^{4,5,6,7}

¹*CQIQC and Department of Physics, University of Toronto,
60 Saint George St., Toronto, ON M5S 1A7, Canada*

²*Hitachi Cambridge Laboratory, J. J. Thomson Ave., Cambridge CB3 0HE, United Kingdom*

³*Cavendish Laboratory, Department of Physics, University of Cambridge, Cambridge CB3 0HE, United Kingdom*

⁴*Joint Center for Quantum Information and Computer Science,
NIST and University of Maryland, College Park, MD 20742, USA*

⁵*Institute for Physical Science and Technology, University of Maryland, College Park, MD 20742, USA*

⁶*ITAMP, Harvard-Smithsonian Center for Astrophysics, Cambridge, MA 02138, USA*

⁷*Department of Physics, Harvard University, Cambridge, MA 02138, USA*

(Dated: March 25, 2022)

Operator noncommutation, a hallmark of quantum theory, limits measurement precision, according to uncertainty principles. Wielded correctly, though, noncommutation can boost precision. A recent foundational result relates a metrological advantage with negative quasiprobabilities—quantum extensions of probabilities—engendered by noncommuting operators. We crystallize the relationship in an equation that we prove theoretically and observe experimentally. Our proof-of-principle optical experiment features a filtering technique that we term *partially postselected amplification* (PPA). Using PPA, we measure a waveplate’s birefringent phase. PPA amplifies, by over two orders of magnitude, the information obtained about the phase per detected photon. In principle, PPA can boost the information obtained from the average filtered photon by an arbitrarily large factor. The filter’s amplification of systematic errors, we find, bounds the theoretically unlimited advantage in practice. PPA can facilitate any phase measurement and mitigates challenges that scale with trial number, such as proportional noise and detector saturation. By quantifying PPA’s metrological advantage with quasiprobabilities, we reveal deep connections between quantum foundations and precision measurement.

Introduction.—Advances in quantum metrology have kindled new measurement techniques [1–5]. The paradigmatic quantum measurement is phase estimation, whose applications span polarimetry, magnetic sensing, gravitational-wave astronomy, and quantum-computer calibration [6–12]. A fundamental limit bounds how precisely one can estimate a phase from a given number of trials [13, 14]. If some trials are filtered out, the average information per retained, or *postselected*, trial can exceed this limit [15]. Filtering can never increase the information per *input* trial, so successful postselections’ rarity counterbalances the extra information [16, 17]. Nevertheless, distilling information from many input trials into fewer postselected trials can alleviate challenges that scale with trial number, including detector saturation, proportional noise, low-frequency noise, limited memory, and limited computational power [18–22].

We elucidate this distillation’s physical and mathematical roots using a filtering technique that we call *partially postselected amplification* (PPA). Theoretically, the information obtained per PPA trial can diverge as the

fraction of postselected trials vanishes [15]. A related technique, weak-value amplification, offers a similarly diverging advantage [18, 20–48]. Both techniques are examples of *noncommutative filtering*. We define *noncommutative filtering* as any filtering whose effect depends on when the filter acts. During the alternative, *commutative filtering*, the per-postselected-trial precision cannot exceed the per-input-trial limit [15]. Examples include the neutral-density filter that reduces a camera’s overexposure. PPA’s postselected trials break the per-input-trial limit by endowing a certain quasiprobability distribution with negative elements [15].

Quasiprobabilities represent quantum states as probability densities represent states in classical statistical mechanics. Like probabilities, the quasiprobabilities in a distribution sum to one. Yet quasiprobabilities can assume negative and nonreal values, called *nonclassical values*. They can arise when the quasiprobability describes quantum-incompatible operations or observables. Well-known quasiprobability distributions include the Wigner function. A rising star is the *Kirkwood-Dirac distribution* [49, 50], which has recently found applications in quantum state tomography [51–55], chaos [56–60], postselected metrology [15, 27, 28, 30, 61–67], measurement disturbance [68–71], quantum thermodynamics [56, 72–75], and quantum foundations [36, 69, 76–87]. Negative Kirkwood-Dirac quasiprobabilities have been demonstrated, under certain conditions, to underlie operational advantages in quantum computation, work extraction, and parameter estimation [15, 58, 67, 75].

* nlupugla@physics.utoronto.ca. The first two coauthors contributed equally.

† ybylmaz@physics.utoronto.ca.

‡ drma2@cam.ac.uk

§ brodutch@physics.utoronto.ca

¶ arthur.pang@mail.utoronto.ca

** steinberg@physics.utoronto.ca

In this Letter, we demonstrate PPA's parameter-estimation enhancement in a proof-of-principle polarimetry experiment. We estimate the birefringent phase imparted to photons by a near-half-waveplate. A tunable polarization filter implements the PPA. The filter boosts the per-detected-photon precision by over two orders of magnitude. Furthermore, we measure a Kirkwood-Dirac distribution that describes the experiment. Our experiment operationally motivates a measure of the distribution's negativity. We prove theoretically and confirm experimentally that the negativity is proportional to the precision enhancement when the phase is probed optimally. We also pinpoint which systematic errors limit PPA's theoretically unbounded precision enhancement (Supplemental Material [88], App. A). Our experiment unifies theoretical quantum foundations with practical precision measurement.

Theoretical background and equality.—Consider estimating a parameter θ by measuring a quantum state $\rho(\theta)$. The *quantum Fisher information* (QFI) $\mathcal{I}(\theta)$ quantifies the information provided by $\rho(\theta)$ about θ , via the state's sensitivity to changes in θ [89] (Supplemental Material [88], App. B). The QFI's reciprocal lower-bounds the variance of every unbiased estimator θ_e of θ , in the Cramér-Rao bound, $\text{var}(\theta_e) \geq 1/\mathcal{I}(\theta)$. [13, 14]

Let A denote an observable with greatest and least eigenvalues a_+ and $a_- = a_+ - \Delta$. The eigenstates $|a_{\pm}\rangle$ satisfy $A|a_{\pm}\rangle = a_{\pm}|a_{\pm}\rangle$. Let a unitary $U(\theta) = \exp(i\theta A)$ imprint θ on an input state. The optimal inputs are even-weight superpositions of extremal A eigenstates, e.g., $|0\rangle = (|a_+\rangle + |a_-\rangle)/\sqrt{2}$ and $|1\rangle = (|a_+\rangle - |a_-\rangle)/\sqrt{2}$. The imprinted state $U(\theta)|0\rangle = |\Psi(\theta)\rangle$ carries the most QFI possible without postselection, $\mathcal{I}(\theta) = \Delta^2$.

A postselected state can provide more QFI. If the angle is small ($\theta\Delta \ll 1$), then $|\Psi(\theta)\rangle \approx |0\rangle + i\frac{\theta\Delta}{2}|1\rangle$. The $|0\rangle$ coefficient is less sensitive to θ than the $|1\rangle$ coefficient, yet $|0\rangle$ has a greater population. PPA partially postselects on $|1\rangle$ via a filter whose $|1\rangle$ transmission amplitude is unity and whose $|0\rangle$ transmission amplitude is parametrically smaller.

More precisely, let t denote the amplitude for $|0\rangle$'s survival of the filter. The filter acts as the Kraus operator [90] $K(t) = t|0\rangle\langle 0| + |1\rangle\langle 1|$, wherein $|t| \in [0, 1]$. For any $|t| < 1$, the filter does not commute with the generator A and enables noncommutative filtering. The filter lets $|\Psi(\theta)\rangle$ pass with a probability

$$p^{\text{ps}}(\theta, t) = \text{Tr}(K(t)|\Psi(\theta)\rangle\langle\Psi(\theta)|K(t)^\dagger) \quad (1)$$

$$= |t|^2 \cos^2(\Delta\theta/2) + \sin^2(\Delta\theta/2). \quad (2)$$

The state becomes

$$|\Psi^{\text{ps}}(\theta, t)\rangle = K(t)|\Psi(\theta)\rangle/\sqrt{p^{\text{ps}}(\theta, t)} \quad (3)$$

$$= \cos(\Delta\theta/2)|0\rangle + i \sin(\Delta\theta/2)|1\rangle. \quad (4)$$

The filter effectively amplifies θ to a Θ defined through $\tan(\Delta\Theta/2) = \tan(\Delta\theta/2)/|t|$. The postselected state carries the QFI

$$\mathcal{I}(\theta) = [\Delta |t|/p^{\text{ps}}(\theta, t)]^2. \quad (5)$$

$\tilde{p}_{\rho(\theta),t}(a, a' +)$	$a' = a_+$	$a' = a_-$
$a = a_+$	$\frac{1+ t ^2}{4p^{\text{ps}}(\theta, t)}$	$e^{i\Delta\theta} \frac{-1+ t ^2}{4p^{\text{ps}}(\theta, t)}$
$a = a_-$	$e^{-i\Delta\theta} \frac{-1+ t ^2}{4p^{\text{ps}}(\theta, t)}$	$\frac{1+ t ^2}{4p^{\text{ps}}(\theta, t)}$

TABLE I: Conditional Kirkwood-Dirac distribution (7) for our PPA experiment and $\rho(\theta) = |\Psi(\theta)\rangle\langle\Psi(\theta)|$.

A large angle is typically easier to observe than a smaller one. If the angle is small, $\Delta\theta \ll 1$, then Θ exceeds θ by a factor of $1/|t|$. This amplification boosts the information obtained per detected state: $\mathcal{I}(\theta) \approx (\Delta/|t|)^2$. The amplification is arbitrarily large if $\Delta\theta$ is arbitrarily small. Such extreme filtering does not significantly reduce the information obtainable per input state: $p^{\text{ps}}(\theta, t)\mathcal{I}(\theta) \approx \Delta^2$, if $\tan(\Delta\theta/2) \ll |t|$.

PPA can be beneficial even if $\Delta\theta$ is large. Suppose prior knowledge indicates that $\theta \approx \theta_p$. Performing $U(-\theta_p)$ after $U(\theta)$ shrinks the probed angle to $\Delta(\theta - \theta_p)$.

Why can a successful PPA trial offer more information than Δ^2 , the most information offered by any input trial? Reference [15] identified a necessary condition. A projectively postselected trial can carry information $> \Delta^2$ only if a Kirkwood-Dirac distribution contains a negative quasiprobability. We generalize that result beyond projective postselection.

Let $\{|a\rangle\}_a$ and $\{|a'\rangle\}_{a'}$ denote copies of an A eigenbasis. Kraus operators $\{K_f\}_f$ with $\sum_f K_f^\dagger K_f = \mathbb{1}$ model the partial postselection. The information-bearing state $\rho(\theta)$ is represented by the Kirkwood-Dirac quasiprobabilities (Supplemental Material [88], App. C)

$$\tilde{p}_{\rho(\theta)}(a, f, a') := \text{Tr}(|a'\rangle\langle a'|K_f^\dagger K_f|a\rangle\langle a|\rho(\theta)). \quad (6)$$

Conditioning on a postselection outcome f induces the *conditional Kirkwood-Dirac distribution*

$$\tilde{p}_{\rho(\theta)}(a, a'|f) := \tilde{p}_{\rho(\theta)}(a, f, a') / \sum_{a,a'} \tilde{p}_{\rho(\theta)}(a, f, a'). \quad (7)$$

These quasiprobabilities are positive if A and $K_f^\dagger K_f$ commute on the support of $\rho(\theta)$ [85].

PPA involves Kraus operators, $K_+ = K(t)$ and $K_- = \sqrt{\mathbb{1} - K(t)^\dagger K(t)}$, that effect successful and unsuccessful postselection. Table I shows PPA's conditional quasiprobabilities, labeled by t , for $\rho(\theta) = |\Psi(\theta)\rangle\langle\Psi(\theta)|$. If $\Delta\theta < \pi$ and $|t| < 1$, the real part of $\tilde{p}_{\rho(\theta),t}(a_{\pm}, a_{\mp}|+)$ is negative, and the postselected QFI (5) exceeds Δ^2 . This concurrence stems from an equality that we prove.

We start by introducing a new measure of Kirkwood-Dirac negativity [58, 85, 86]. Let x denote the vector of arguments for a Kirkwood-Dirac distribution $\{\tilde{p}(x)\}_x$. Define the *nonclassicality gap* as the greatest difference between quasiprobabilities' absolute squares: $\max_x \{|\tilde{p}(x)|^2\} - \min_x \{|\tilde{p}(x)|^2\}$. The gap > 1 only if a quasiprobability $\notin [0, 1]$. For any postselection operator

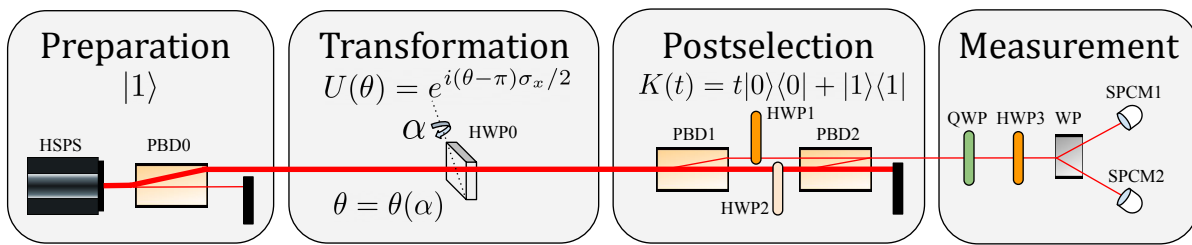


FIG. 1: Photonic parameter-estimation experiment: Preparation: A heralded–single–photon source (HSPS) emits light that hits a polarizing–beam–displacer (PBD0) and emerges vertically polarized ($|1\rangle$). Transformation: The half-waveplate (HWP0) has an optic axis angled 45° above the horizontal. HWP0 is tilted away from normal incidence through an angle α about its optic axis. The waveplate rotates a photon’s polarization through an angle $\theta(\alpha) - \pi$. A calibration curve of $\theta(\alpha) \equiv \theta$ provides a prior estimate of θ . We use this estimate to calculate the polarization projection optimal for inferring θ (Supplemental Material [88], App. B). Postselection: A polarizing–beam–displacer interferometer, followed by a beam block in the undisplaced port, realizes a partial polarizer. The horizontal-polarization transmission amplitude, t with $|t| \in [0, 1]$, is controlled by a half-waveplate (HWP2) inside the interferometer. The filter discards all horizontally polarized photons when $|t| = 0$ and none when $|t| = 1$. Measurement: Motorized waveplates, followed by a Wollaston prism (WP) and single-photon counter modules (SPCM), project onto any desired polarization.

K_+ , the nonclassicality gap is proportional to the optimal input state’s postselected QFI (Supplemental Material [88], App. D):

$$\mathcal{I}(\theta) = 4 \Delta^2 \times \left[\max_{a, a'} \{ |\tilde{p}_{\rho(\theta)}(a, a' | +) |^2 \} - \min_{a, a'} \{ |\tilde{p}_{\rho(\theta)}(a, a' | +) |^2 \} \right]. \quad (8)$$

Equation (8) crystallizes the relationship between postselected quantum metrology and Kirkwood-Dirac nonclassicality.

Experimental setup.—We realize PPA in a proof-of-principle polarimetry experiment (Fig. 1). The to-be-estimated parameter θ is the excess birefringent phase, beyond π , imparted by a near-half-waveplate (HWP0). A heralded–single–photon source emits vertically polarized photons with wavelengths of 808 nm. The photons hit HWP0, whose optic axis lies 45° above the horizontal. Tilting HWP0 through an incidence angle α sets its birefringent retardance to $\theta(\alpha) - \pi$. A calibration curve of $\theta(\alpha) \equiv \theta$ provides prior knowledge about θ .

Denote horizontal polarization by $|0\rangle$; and vertical polarization, by $|1\rangle$. We filter the photons by attenuating one polarization, using an interferometer formed from polarizing beam displacers. The postselection parameter t equals the filter’s ($|0\rangle$ transmission amplitude)/($|1\rangle$ transmission amplitude). We control t with a motorized waveplate (HWP2) placed in the interferometer.

HWP0 rotates the photon’s polarization with the unitary $\exp(i[\theta - \pi]\sigma_x/2)$. The generator $A = \sigma_x/2$ has eigenvalues $a_{\pm} = \pm 1/2$ and eigenstates $|a_{\pm}\rangle = (|0\rangle \pm |1\rangle)/\sqrt{2}$. The filtered photons occupy the state $\rho^{\text{ps}}(\theta, t)$ —ideally, the pure state (4). We projectively measure the state’s polarization to estimate θ .

Experimental results.—First, we assess PPA’s metrological performance. Then, we present the measured quasiprobabilities (7). Comparing the quasiprobabilities with the QFI, we support Eq. (8) experimentally.

Polarization tomography reveals how PPA boosts sensitivity. Figure 2a shows the postselected state’s amplified angle, Θ , versus the true θ value. We infer the latter using state tomography without postselection ($|t| = 1$). The slope of $\Theta(\theta)$ quantifies our sensitivity to small changes in θ . When $|t| = 1$, $\Theta(\theta)$ has a unit slope. As we postselect more ($|t|$ decreases), the slope grows—by a factor of > 20 at $|t| = 0.044$.

We estimate θ by projectively measuring many copies of the amplified state identically. The measurement basis is optimized to provide the QFI according to calibrations of $\theta(\alpha)$ and t (Supplemental Material [88], App. B).

For each (θ, t) , we sample 32 independent estimates of θ . Figure 2b displays our estimates’ precision and accuracy, normalized by the number N of detected photons. The precision per photon, $\text{var}(\theta_e)^{-1}/N$, agrees excellently with the QFI (5). The accuracy per photon, $\text{MSE}(\theta_e)^{-1}/N$, mostly agrees with the QFI but falls short at the smallest θ and $|t|$. The per-photon precision enhancement maximizes at 540 ± 150 , when $\theta = 0.040$ rad, $|t| = 0.044$. The per-photon accuracy caps at 78 ± 15 , when $\theta = 0.116$ rad and $|t| = 0.082$.

The discrepancy between precision and accuracy arises because PPA amplifies systematic errors (Supplemental Material [88], App. A). Small errors in adjusting the waveplates that set $|t|$ or A produce systematic error. These errors begin to dominate the statistical noise as the amplification increases. Remarkably, we found the amplified errors helpful for detecting and correcting errors in A that went unnoticed without PPA’s amplification.

We extract the conditional quasiprobabilities (6) from tomography of the unpostselected ($|t| = 1$) state and present them in Fig. 3. At each (θ, t) , the sum over the quasiprobabilities is normalized to one. When $|t| < 1$, quasiprobabilities acquire negative real parts, so other quasiprobabilities acquire real parts > 1 to ensure a unit sum. As $|t|$ decreases, elements’ magnitudes increase—to > 70 at the smallest θ and $|t|$.

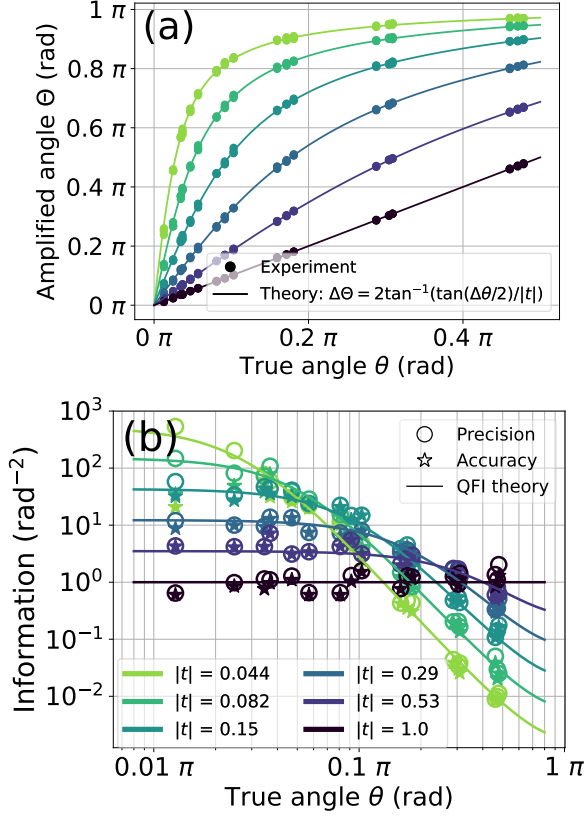


FIG. 2: Experimental performance of PPA with different magnitudes of postsselection parameter, $|t|$. (a) Amplified angle vs. true angle θ . The slope signifies sensitivity to changes in θ . When θ is small [$\tan(\Delta\theta/2) \ll |t|$], PPA magnifies θ by a factor of $1/|t|$. Setting $|t| = \tan(\Delta\theta/2)$ amplifies θ to $\pi/2$ and optimizes the sensitivity. Decreasing $|t|$ further reduces the sensitivity, rendering prior knowledge about θ important. (b) Information per photon vs. θ . For each $(\theta, |t|)$, we make 32 independent estimates of θ and display the estimates’ precision ($1/\text{variance}$) and accuracy ($1/[\text{mean squared error}]$) per mean detected photon. The per-photon precision agrees with the predicted QFI (5) and climbs to $540 \pm 150 \text{ rad}^{-2}$ at $(\theta, |t|) = (0.040 \text{ rad}, 0.044)$. The per-photon accuracy suffers from systematic errors at the smallest θ and $|t|$, yet still reaches $78 \pm 15 \text{ rad}^{-2}$ at $(\theta, |t|) = (0.116 \text{ rad}, 0.082)$.

Figure 4 compares the nonclassicality gap with the QFI. We compute the gap from the quasiprobabilities shown in Fig. 3. The estimated gap is the arithmetic mean over four runs of tomography. We determine the QFI at $\theta = \theta_0$ empirically from estimates of $\rho^{\text{ps}}(\theta_0, t)$ and $\partial\rho^{\text{ps}}(\theta, t)/\partial\theta|_{\theta_0}$ (Supplemental Material [88], App. B states the formula for QFI). The derivative is the matrix slope of a linear fit through three tomographic estimates: $\rho^{\text{ps}}(\theta_0 - d\theta, t)$, $\rho^{\text{ps}}(\theta_0, t)$, and $\rho^{\text{ps}}(\theta_0 + d\theta, t)$; $d\theta = 0.035$ radians. We repeat the procedure over four tomographic runs to obtain a distribution of QFIs at each $(\theta, |t|)$. Empirically, the distribution of the QFIs is approximately log-normal, so we estimate the QFI and its uncertainty using the geometric mean and geometric standard error.

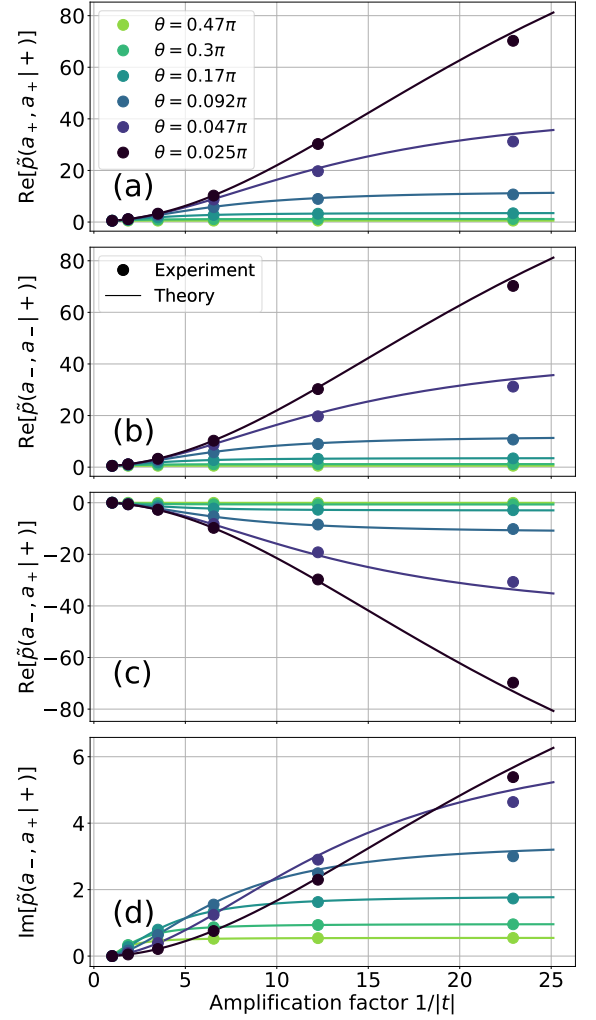


FIG. 3: Quasiprobabilities vs. amplification factor $1/|t|$. We inferred the Kirkwood-Dirac distribution (6), $\tilde{\rho}_{\rho(\theta), t}(a, a' | +)$, from tomography of the unpostselected ($|t| = 1$) state. We present empirical results together with theoretical predictions at different θ and $|t|$ for select elements: (a) $\text{Re}[\tilde{\rho}_{\rho(\theta), t}(a_+, a_+ | +)]$, (b) $\text{Re}[\tilde{\rho}_{\rho(\theta), t}(a_-, a_- | +)]$, (c) $\text{Re}[\tilde{\rho}_{\rho(\theta), t}(a_-, a_+ | +)]$, and (d) $\text{Im}[\tilde{\rho}_{\rho(\theta), t}(a_-, a_+ | +)]$. All other elements are redundant because (6) ensures $\tilde{\rho}_{\rho(\theta), t}(a, a' | +) = \tilde{\rho}_{\rho(\theta), t}(a', a | +)^*$. For each $(\theta, |t|)$, the quasiprobabilities’ sum is normalized to 1. Negativity in $\text{Re}[\tilde{\rho}_{\rho(\theta), t}(a_{\pm}, a_{\mp} | +)]$ allows the magnitude of each element to be greater than 1. The negativity increases as the amplification strengthens.

The estimated QFI and nonclassicality gap are consistent with the theoretical QFI [Fig. 4(a)]. Thus, our experiment corroborates the relationship (8) between enhanced precision and quasiprobability negativity.

Conclusions.—We have experimentally demonstrated and theoretically proved how negative Kirkwood-Dirac quasiprobabilities enhance postselected metrology. We introduced and illustrated a scheme for phase estimation, partially postselected amplification. In our polarimetry experiment, PPA boosted our per-detected-photon pre-

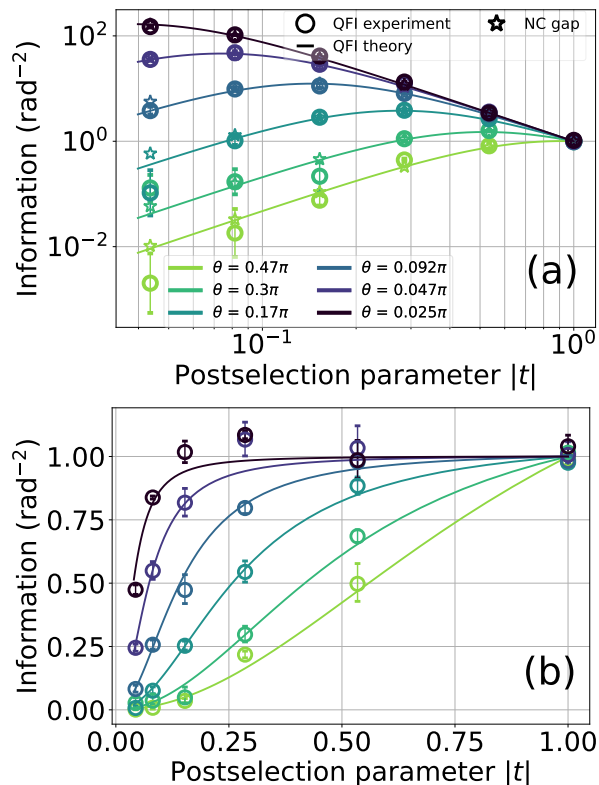


FIG. 4: Information per detected photon (a) and per input photon (b) vs. magnitude of postselection parameter, $|t|$. Error bars denote the geometric standard error of 4 independent runs. The experimental QFI and 4 times the nonclassicality gap are within error of the theoretical QFI (5). Without postselection, our estimates are shot-noise-limited to the per-input-photon precision 1 rad^{-2} . As we increasingly postselect (as $|t|$ decreases), the per-detected-photon precision increases when $\theta \approx 0$ and decreases when $\tan(\theta/2) < |t|$. The smallest $|t|$ and θ provide a per-detected-photon precision $> 200 \text{ rad}^{-2}$, despite sacrificing little per-input-photon precision.

recision by over two orders of magnitude. This enhancement derives from negativity of a generalized Kirkwood-Dirac quasiprobability, according to an equation that we prove and experimentally support. The negativity demonstrates that our filter provides a benefit offered by no filter that commutes with $U(\theta)$.

In theory, PPA's precision boost is unbounded. In practice, we find, the phase amplification augments systematic errors. Yet the error amplification has a silver lining, having helped us detect and correct systematic errors in our implementation of the generator A (Supplemental Material [88], App. A).

PPA is related to weak-value amplification (WVA), a scheme for estimating couplings strengths [18, 20–48]. PPA and WVA concentrate information spread across many input trials into few postselected trials. Yet PPA differs from WVA in three ways: (i) PPA can amplify any phase, not just coupling strengths. (ii) PPA sur-

vives decoherence better. In WVA, an interaction couples two systems. One system is measured, the other is postselected, and both must remain coherent during the interaction. PPA only requires the measured system to maintain coherence. (iii) PPA admits of a simpler mathematical treatment: WVA requires a Hilbert-space dimensionality ≥ 4 , whereas PPA works with a Hilbert-space dimensionality ≥ 2 . PPA is therefore a promising tool for combating metrological challenges that scale with the number of completed trials. As a whole, our work interweaves the disparate studies of precision measurement and quantum foundations.

ACKNOWLEDGMENTS

We thank Justin Dressel, Hugo Ferretti, Kent Fisher, Zhaokai Li, Seth Lloyd, and Edwin Tham for helpful conversations. This work was supported by the Natural Sciences and Engineering Research Council (NSERC) of Canada, the National Science Foundation under Grant No. NSF PHY-1748958, the EPSRC, CIFAR, Lars Hierta's Memorial Foundation, and Girton College. It made use of some equipment purchased through grant FQXiRFP-1819 from the Foundational Questions Institute and Fetzer Franklin Fund, a donor advised fund of Silicon Valley Community Foundation. A.M.S is a fellow of CIFAR, and N.Y.H is grateful for an NSF grant for the Institute for Theoretical Atomic, Molecular, and Optical Physics at Harvard University and the Smithsonian Astrophysical Observatory.

REFERENCES

- [1] L. A. Rozema, A. Darabi, D. H. Mahler, A. Hayat, Y. Soudagar, and A. M. Steinberg, Violation of heisenberg's measurement-disturbance relationship by weak measurements, *Phys. Rev. Lett.* **109**, 100404 (2012).
- [2] V. Giovannetti, S. Lloyd, and L. Maccone, Quantum-enhanced measurements: beating the standard quantum limit, *Science* **306**, 1330 (2004).
- [3] V. Giovannetti, S. Lloyd, and L. Maccone, Quantum metrology, *Physical review letters* **96**, 010401 (2006).
- [4] V. Giovannetti, S. Lloyd, and L. Maccone, Advances in quantum metrology, *Nature photonics* **5**, 222 (2011).
- [5] E. Polino, M. Valeri, N. Spagnolo, and F. Sciarrino, Photonic quantum metrology, *AVS Quantum Science* **2**, 024703 (2020), <https://doi.org/10.1116/5.0007577>.
- [6] S.-J. Yoon, J.-S. Lee, C. Rockstuhl, C. Lee, and K.-G. Lee, Experimental quantum polarimetry using heralded single photons, *Metrologia* **57**, 045008 (2020).
- [7] J. Abadie *et al.* (LIGO Scientific Collaboration), A gravitational wave observatory operating beyond the quantum shot-noise limit, *Nature Physics* 2011 7:12 **7**, 962 (2011).
- [8] B. P. Abbott *et al.* (LIGO Scientific Collaboration and Virgo Collaboration), Observation of gravitational waves from a binary black hole merger, *Phys. Rev. Lett.* **116**, 061102 (2016).
- [9] N. Ghosh and A. I. Vitkin, Tissue polarimetry: concepts,

- challenges, applications, and outlook, *Journal of biomedical optics* **16**, 110801 (2011).
- [10] D. Budker and M. Romalis, Optical magnetometry, *Nature physics* **3**, 227 (2007).
- [11] E. Knill, D. Leibfried, R. Reichle, J. Britton, R. B. Blakestad, J. D. Jost, C. Langer, R. Ozeri, S. Seidelin, and D. J. Wineland, Randomized benchmarking of quantum gates, *Physical Review A* **77**, 012307 (2008).
- [12] M. Dobšíček, G. Johansson, V. Shumeiko, and G. Wendin, Arbitrary accuracy iterative quantum phase estimation algorithm using a single ancillary qubit: A two-qubit benchmark, *Physical Review A* **76**, 030306(R) (2007).
- [13] H. Cramér, *Mathematical methods of statistics (PMS-9)*, Vol. 9 (Princeton University Press, 2016).
- [14] C. R. Rao, Information and the accuracy attainable in the estimation of statistical parameters, in *Breakthroughs in statistics* (Springer, 1992) pp. 235–247.
- [15] D. R. M. Arvidsson-Shukur, N. Yunger Halpern, H. V. Lepage, A. A. Lasek, C. H. W. Barnes, and S. Lloyd, Quantum advantage in postselected metrology, *Nature Communications* **11**, 3775 (2020).
- [16] J. Combes, C. Ferrie, Z. Jiang, and C. M. Caves, Quantum limits on postselected, probabilistic quantum metrology, *Phys. Rev. A* **89**, 052117 (2014).
- [17] C. Ferrie and J. Combes, Weak value amplification is suboptimal for estimation and detection, *Phys. Rev. Lett.* **112**, 040406 (2014).
- [18] J. Harris, R. W. Boyd, and J. S. Lundeen, Weak value amplification can outperform conventional measurement in the presence of detector saturation, *Phys. Rev. Lett.* **118**, 070802 (2017).
- [19] J. Sinclair, M. Hallaji, A. M. Steinberg, J. Tollaksen, and A. N. Jordan, Weak-value amplification and optimal parameter estimation in the presence of correlated noise, *Phys. Rev. A* **96**, 052128 (2017).
- [20] M. Hallaji, A. Feizpour, G. Dmochowski, J. Sinclair, and A. M. Steinberg, Weak-value amplification of the nonlinear effect of a single photon, *Nature Physics* **13**, 540 (2017).
- [21] G. I. Viza, J. Martínez-Rincón, G. B. Alves, A. N. Jordan, and J. C. Howell, Experimentally quantifying the advantages of weak-value-based metrology, *Phys. Rev. A* **92**, 032127 (2015).
- [22] X. Qiu, L. Xie, X. Liu, L. Luo, Z. Li, Z. Zhang, and J. Du, Precision phase estimation based on weak-value amplification, *Applied Physics Letters* **110**, 071105 (2017).
- [23] Y. Aharonov, D. Z. Albert, and L. Vaidman, How the result of a measurement of a component of the spin of a spin- $1/2$ particle can turn out to be 100, *Phys. Rev. Lett.* **60**, 1351 (1988).
- [24] I. M. Duck, P. M. Stevenson, and E. C. G. Sudarshan, The sense in which a “weak measurement” of a spin- $1/2$ particle’s spin component yields a value 100, *Phys. Rev. D* **40**, 2112 (1989).
- [25] O. Hosten and P. Kwiat, Observation of the spin hall effect of light via weak measurements, *Science* **319**, 787 (2008).
- [26] P. B. Dixon, D. J. Starling, A. N. Jordan, and J. C. Howell, Ultrasensitive beam deflection measurement via interferometric weak value amplification, *Phys. Rev. Lett.* **102**, 173601 (2009).
- [27] S. Pang, J. Dressel, and T. A. Brun, Entanglement-assisted weak value amplification, *Phys. Rev. Lett.* **113**, 030401 (2014).
- [28] S. Pang and T. A. Brun, Improving the precision of weak measurements by postselection measurement, *Phys. Rev. Lett.* **115**, 120401 (2015).
- [29] A. N. Jordan, J. Martínez-Rincón, and J. C. Howell, Technical advantages for weak-value amplification: when less is more, *Physical Review X* **4**, 011031 (2014).
- [30] D. J. Starling, P. B. Dixon, A. N. Jordan, and J. C. Howell, Optimizing the signal-to-noise ratio of a beam-deflection measurement with interferometric weak values, *Phys. Rev. A* **80**, 041803(R) (2009).
- [31] D. J. Starling, P. B. Dixon, A. N. Jordan, and J. C. Howell, Precision frequency measurements with interferometric weak values, *Phys. Rev. A* **82**, 063822 (2010).
- [32] O. S. Magaña-Loaiza, M. Mirhosseini, B. Rodenburg, and R. W. Boyd, Amplification of angular rotations using weak measurements, *Phys. Rev. Lett.* **112**, 200401 (2014).
- [33] K. Lyons, J. Dressel, A. N. Jordan, J. C. Howell, and P. G. Kwiat, Power-recycled weak-value-based metrology, *Phys. Rev. Lett.* **114**, 170801 (2015).
- [34] J. Martínez-Rincón, C. A. Mullarkey, G. I. Viza, W.-T. Liu, and J. C. Howell, Ultrasensitive inverse weak-value tilt meter, *Opt. Lett.* **42**, 2479 (2017).
- [35] P. Egan and J. A. Stone, Weak-value thermostat with 0.2 mk precision, *Opt. Lett.* **37**, 4991 (2012).
- [36] H. F. Hofmann, M. E. Goggin, M. P. Almeida, and M. Barbieri, Estimation of a quantum interaction parameter using weak measurements: Theory and experiment, *Phys. Rev. A* **86**, 040102(R) (2012).
- [37] Y. Kim, Y.-S. Kim, S.-Y. Lee, S.-W. Han, S. Moon, Y.-H. Kim, and Y.-W. Cho, Direct quantum process tomography via measuring sequential weak values of incompatible observables, *Nature communications* **9**, 1 (2018).
- [38] M. Pfender, P. Wang, H. Sumiya, S. Onoda, W. Yang, D. B. R. Dasari, P. Neumann, X.-Y. Pan, J. Isoya, R.-B. Liu, *et al.*, High-resolution spectroscopy of single nuclear spins via sequential weak measurements, *Nature communications* **10**, 1 (2019).
- [39] F. Piacentini, A. Avella, M. P. Levi, M. Gramegna, G. Brida, I. P. Degiovanni, E. Cohen, R. Lussana, F. Villa, A. Tosi, F. Zappa, and M. Genovese, Measuring incompatible observables by exploiting sequential weak values, *Phys. Rev. Lett.* **117**, 170402 (2016).
- [40] L. Diósi, Structural features of sequential weak measurements, *Physical Review A* **94**, 010103(R) (2016).
- [41] A. Avella, F. Piacentini, M. Borsarelli, M. Barbieri, M. Gramegna, R. Lussana, F. Villa, A. Tosi, I. P. Degiovanni, and M. Genovese, Anomalous weak values and the violation of a multiple-measurement leggett-garg inequality, *Physical Review A* **96**, 052123 (2017).
- [42] D. Georgiev and E. Cohen, Probing finite coarse-grained virtual feynman histories with sequential weak values, *Physical Review A* **97**, 052102 (2018).
- [43] H. F. Hofmann, Contextuality of quantum fluctuations characterized by conditional weak values of entangled states, *Physical Review A* **102**, 062215 (2020).
- [44] G. Foletto, M. Padovan, M. Avesani, H. Tebyanian, P. Villoresi, and G. Vallone, Experimental test of sequential weak measurements for certified quantum randomness extraction, *Phys. Rev. A* **103**, 062206 (2021).
- [45] J.-S. Chen, M.-J. Hu, X.-M. Hu, B.-H. Liu, Y.-F. Huang, C.-F. Li, C.-G. Guo, and Y.-S. Zhang, Experimental realization of sequential weak measurements of non-

- commuting pauli observables, *Opt. Express* **27**, 6089 (2019).
- [46] V. Cimini, I. Gianani, F. Piacentini, I. P. Degiovanni, and M. Barbieri, Anomalous values, fisher information, and contextuality, in generalized quantum measurements, *Quantum Science and Technology* **5**, 025007 (2020).
- [47] Y.-H. Choi, S. Hong, T. Pramanik, H.-T. Lim, Y.-S. Kim, H. Jung, S.-W. Han, S. Moon, and Y.-W. Cho, Demonstration of simultaneous quantum steering by multiple observers via sequential weak measurements, *Optica* **7**, 675 (2020).
- [48] M. Blok, C. Bonato, M. Markham, D. Twitchen, V. Dobrovitski, and R. Hanson, Manipulating a qubit through the backaction of sequential partial measurements and real-time feedback, *Nature Physics* **10**, 189 (2014).
- [49] J. G. Kirkwood, Quantum statistics of almost classical assemblies, *Phys. Rev.* **44**, 31 (1933).
- [50] P. A. M. Dirac, On the analogy between classical and quantum mechanics, *Rev. Mod. Phys.* **17**, 195 (1945).
- [51] L. M. Johansen, Quantum theory of successive projective measurements, *Phys. Rev. A* **76**, 012119 (2007).
- [52] J. S. Lundeen, B. Sutherland, A. Patel, C. Stewart, and C. Bamber, Direct measurement of the quantum wavefunction, *Nature* **474**, 188 (2011).
- [53] J. S. Lundeen and C. Bamber, Procedure for direct measurement of general quantum states using weak measurement, *Phys. Rev. Lett.* **108**, 070402 (2012).
- [54] C. Bamber and J. S. Lundeen, Observing dirac's classical phase space analog to the quantum state, *Phys. Rev. Lett.* **112**, 070405 (2014).
- [55] G. S. Thekkadath, L. Giner, Y. Chalich, M. J. Horton, J. Banker, and J. S. Lundeen, Direct measurement of the density matrix of a quantum system, *Phys. Rev. Lett.* **117**, 120401 (2016).
- [56] N. Yunger Halpern, Jarzynski-like equality for the out-of-time-ordered correlator, *Phys. Rev. A* **95**, 012120 (2017).
- [57] N. Yunger Halpern, B. Swingle, and J. Dressel, Quasiprobability behind the out-of-time-ordered correlator, *Phys. Rev. A* **97**, 042105 (2018).
- [58] J. R. González Alonso, N. Yunger Halpern, and J. Dressel, Out-of-time-ordered-correlator quasiprobabilities robustly witness scrambling, *Phys. Rev. Lett.* **122**, 040404 (2019).
- [59] N. Y. Halpern, A. Bartolotta, and J. Pollack, Entropic uncertainty relations for quantum information scrambling, *Communications Physics* **2**, 1 (2019).
- [60] R. Mohseninia, J. R. González Alonso, and J. Dressel, Optimizing measurement strengths for qubit quasiprobabilities behind out-of-time-ordered correlators, *Phys. Rev. A* **100**, 062336 (2019).
- [61] A. M. Steinberg, Conditional probabilities in quantum theory and the tunneling-time controversy, *Phys. Rev. A* **52**, 32 (1995).
- [62] J. Dressel, M. Malik, F. M. Miatto, A. N. Jordan, and R. W. Boyd, Colloquium: Understanding quantum weak values: Basics and applications, *Rev. Mod. Phys.* **86**, 307 (2014).
- [63] M. F. Pusey, Anomalous weak values are proofs of contextuality, *Phys. Rev. Lett.* **113**, 200401 (2014).
- [64] D. R. M. Arvidsson-Shukur, A. N. O. Gottfries, and C. H. W. Barnes, Evaluation of counterfactuality in counterfactual communication protocols, *Phys. Rev. A* **96**, 062316 (2017).
- [65] D. R. M. Arvidsson-Shukur and C. H. W. Barnes, Post-selection and counterfactual communication, *Phys. Rev. A* **99**, 060102(R) (2019).
- [66] R. Kunjwal, M. Lostaglio, and M. F. Pusey, Anomalous weak values and contextuality: Robustness, tightness, and imaginary parts, *Phys. Rev. A* **100**, 042116 (2019).
- [67] J. H. Jenne and D. R. M. Arvidsson-Shukur, Quantum learnability is arbitrarily distillable, arXiv preprint arXiv:1909.11116 (2021).
- [68] R. Jozsa, Complex weak values in quantum measurement, *Phys. Rev. A* **76**, 044103 (2007).
- [69] H. F. Hofmann, On the role of complex phases in the quantum statistics of weak measurements, *New Journal of Physics* **13**, 103009 (2011).
- [70] J. Dressel and A. N. Jordan, Significance of the imaginary part of the weak value, *Phys. Rev. A* **85**, 012107 (2012).
- [71] J. T. Monroe, N. Yunger Halpern, T. Lee, and K. W. Murch, Weak measurement of a superconducting qubit reconciles incompatible operators, *Phys. Rev. Lett.* **126**, 100403 (2021).
- [72] A. E. Allahverdyan, Nonequilibrium quantum fluctuations of work, *Phys. Rev. E* **90**, 032137 (2014).
- [73] H. J. D. Miller and J. Anders, Time-reversal symmetric work distributions for closed quantum dynamics in the histories framework, *New Journal of Physics* **19**, 062001 (2017).
- [74] A. Levy and M. Lostaglio, A quasiprobability distribution for heat fluctuations in the quantum regime, arXiv preprint arXiv:1909.11116 (2019).
- [75] M. Lostaglio, Certifying quantum signatures in thermodynamics and metrology via contextuality of quantum linear response, *Phys. Rev. Lett.* **125**, 230603 (2020).
- [76] R. B. Griffiths, Consistent histories and the interpretation of quantum mechanics, *Journal of Statistical Physics* **36**, 219 (1984).
- [77] S. Goldstein and D. N. Page, Linearly positive histories: Probabilities for a robust family of sequences of quantum events, *Phys. Rev. Lett.* **74**, 3715 (1995).
- [78] J. B. Hartle, Linear positivity and virtual probability, *Phys. Rev. A* **70**, 022104 (2004).
- [79] H. F. Hofmann, Complex joint probabilities as expressions of reversible transformations in quantum mechanics, *New Journal of Physics* **14**, 043031 (2012).
- [80] H. F. Hofmann, Derivation of quantum mechanics from a single fundamental modification of the relations between physical properties, *Phys. Rev. A* **89**, 042115 (2014).
- [81] H. F. Hofmann, Quantum paradoxes originating from the nonclassical statistics of physical properties related to each other by half-periodic transformations, *Phys. Rev. A* **91**, 062123 (2015).
- [82] H. F. Hofmann, On the fundamental role of dynamics in quantum physics, *The European Physical Journal D* **70**, 118 (2016).
- [83] J. J. Halliwell, Leggett-garg inequalities and no-signaling in time: A quasiprobability approach, *Phys. Rev. A* **93**, 022123 (2016).
- [84] B. C. Stacey, Quantum theory as symmetry broken by vitality, arXiv preprint arXiv:1907.02432 (2019).
- [85] D. R. M. Arvidsson-Shukur, J. Chevalier Drori, and N. Yunger Halpern, Conditions tighter than noncommutation needed for nonclassicality, *Journal of Physics A: Mathematical and Theoretical* **54**, 284001 (2021).
- [86] S. De Bievre, Kirkwood-Dirac nonclassicality, support uncertainty and complete incompatibility, arXiv e-prints, arXiv:2106.10017 (2021), arXiv:2106.10017 [quant-ph].

- [87] M. Oszmaniec, D. J. Brod, and E. F. Galvão, Measuring relational information between quantum states, and applications, arXiv e-prints , arXiv:2109.10006 (2021), arXiv:2109.10006 [quant-ph].
- [88] See supplementary material at [URL will be inserted by publisher] for details on systematic errors, optimal measurements, our Kirkwood-Dirac distribution, and proof equating nonclassicality gap with metrological advantage. The supplementary materials include Ref. [91].
- [89] S. L. Braunstein and C. M. Caves, Statistical distance and the geometry of quantum states, *Phys. Rev. Lett.* **72**, 3439 (1994).
- [90] M. A. Nielsen and I. L. Chuang, *Quantum Computation and Quantum Information: 10th Anniversary Edition*, 10th ed. (Cambridge University Press, New York, NY, USA, 2011).
- [91] H. M. Wiseman, Weak values, quantum trajectories, and the cavity-qed experiment on wave-particle correlation, *Phys. Rev. A* **65**, 032111 (2002).